

A Linear-Complexity Finite-Element-Based Eigenvalue Solver for Efficient Analysis of 3-D On-Chip Integrated Circuits

Jongwon Lee, *Student Member, IEEE*, Venkataramanan Balakrishnan, *Fellow, IEEE*, Cheng-Kok Koh, *Senior Member, IEEE*, and Dan Jiao, *Senior Member, IEEE*

Abstract—This letter presents a linear-complexity finite-element-based eigenvalue solver for efficient analysis of 3-D on-chip integrated circuits. In this solver, from the original 3-D quadratic eigenvalue problem governing the on-chip circuits, we formulate a new generalized eigenvalue problem to efficiently compute the eigenvalues and eigenvectors of physical interest. We also develop an efficient linear-complexity solution for the matrix equation involved in the solution of the generalized eigenvalue problem. Numerical results demonstrate the accuracy and efficiency of the proposed eigenvalue solver.

Index Terms—Eigenvalue solver, finite element method, generalized eigenvalue problem, quadratic eigenvalue problem.

I. INTRODUCTION

ANY problems arising from the electromagnetics-based analysis of integrated circuits can be formulated as a complex-valued generalized eigenvalue problem $\mathbf{A}x = \lambda\mathbf{B}x$ [1]–[3]. The computational complexity of a traditional QR-based eigenvalue solver is $O(N^3)$ [4], with N being the size of \mathbf{A} or \mathbf{B} . This complexity can be reduced to $O(N^2)$ by using Arnoldi-based algorithms [2], [4]. In [1], the computational bottleneck in an Arnoldi-based 3-D generalized eigenvalue solution is overcome by a linear-complexity direct solution via the orthogonal prism vector basis functions. Without sacrificing accuracy, the eigenvalue solver in [1] has shown a clear advantage over state-of-the-art eigenvalue solvers in fast CPU time. The solver is efficient for finding k largest eigenvalues of interest. However, to find other arbitrary k eigenvalues of interest, the method in [1] may take many more than $O(k)$ Arnoldi iteration steps, which becomes inefficient. In practice, the largest eigenvalues may not be the eigenvalues of physical interest. For example, in on-chip circuits, due to its working frequency band, the physically important eigenvalues are, in fact, the eigenvalues having the smallest modulus. One can use the shift-inverting technique like that in [2] to shift the eigenvalue spectrum. However, the resultant system matrix equation does not permit a linear-complexity solution described in [1] since the matrix becomes indefinite instead of being positive-definite. To overcome

the aforementioned problem of [1], in this letter, we develop a new eigenvalue solver to find the eigenvalues and eigenvectors of physical interest in a much reduced number of Arnoldi steps, while preserving the linear complexity of the eigenvalue solution. In this solver, we formulate a new generalized eigenvalue problem for analyzing 3-D on-chip integrated circuits. We then develop an efficient preconditioned iterative solution to solve the resultant indefinite system matrix involved in the generalized eigenvalue solution. This efficient solution is enabled by a new preconditioner that renders the spectral radius of the preconditioned matrix small, and also bounded by a constant irrespective of the problem size. As a result, the number of iterations required in the Generalized Minimal Residual (GMRES)-based iterative solution [4] is shown to be a constant, holding the complexity of the entire eigenvalue solution linear.

II. FORMULATION

A. Formulation of a New Generalized Eigenvalue Problem

The quadratic eigenvalue problem governing an arbitrary on-chip integrated circuit containing lossy conductors and inhomogeneous dielectrics can be converted to the following generalized eigenvalue problem [1]:

$$\begin{bmatrix} -\mathbf{S} & \mathbf{0} \\ \mathbf{0} & \mathbf{T} \end{bmatrix} x = \lambda \begin{bmatrix} \mathbf{R} & \mathbf{T} \\ \mathbf{T} & \mathbf{0} \end{bmatrix} x \quad (1)$$

where \mathbf{S} , \mathbf{T} , and \mathbf{R} are, respectively, the stiffness matrix, the mass matrix, and the conductivity-related matrix formulated from a finite-element based method. The λ represents the eigenvalue, and the x denotes the eigenvector of (1).

To expedite the Arnoldi process for finding the eigenvalue solutions of physical interest from (1), we propose to use the conformal mapping technique to cluster the eigenvalues λ into a unit circle and apply the shift-inverting technique to shift the eigenvalue spectrum. We hence transform (1) to

$$\begin{bmatrix} \mathbf{R} + \mathbf{S} & \mathbf{T} \\ \mathbf{T} & -\mathbf{T} \end{bmatrix} x = \lambda' \begin{bmatrix} (-1-\tau)\mathbf{S} + (1-\tau)\mathbf{R} & (1-\tau)\mathbf{T} \\ (1-\tau)\mathbf{T} & (1+\tau)\mathbf{T} \end{bmatrix} x$$

which can be rewritten as

$$\mathbf{A}'x = \lambda'\mathbf{B}'x \quad (2)$$

in which $\lambda' = 1/\{(1+\lambda)/(1-\lambda) - \tau\}$ and τ is the initial guess of $(1+\lambda)/(1-\lambda)$. In an Arnoldi-based eigenvalue solution [4], The essential computation of (2) is the matrix-vector multiplication $\mathbf{B}'^{-1}\mathbf{A}'x'$, where x' is a vector that is initialized to be an arbitrary nonzero vector, and then updated to another vector at every Arnoldi step. Denote $\mathbf{A}'x'$ by q , which can be obtained

Manuscript received July 23, 2014; accepted September 19, 2014. Date of publication October 24, 2014; date of current version December 01, 2014. This work was supported by a grant from Intel Corporation, a grant from DARPA under award HR0011-14-1-0057, and a grant from the NSF under award 1065318.

The authors are with the School of Electrical and Computer Engineering, Purdue University, West Lafayette, IN 47906 USA (e-mail: djiao@purdue.edu).

Color versions of one or more of the figures in this paper are available online at <http://ieeexplore.ieee.org>.

Digital Object Identifier 10.1109/LMWC.2014.2361677

in linear complexity since \mathbf{A}' is sparse. Let q be $\{q_1 q_2\}^T$, the $\mathbf{B}'^{-1}q$ can then be computed with the inversion lemma [5] as

$$\mathbf{B}'^{-1} \begin{Bmatrix} q_1 \\ q_2 \end{Bmatrix} = \begin{Bmatrix} \mathbf{S}_1^{-1} \left(q_1 - \frac{1-\tau}{1+\tau} q_2 \right) \\ -\frac{1-\tau}{1+\tau} \mathbf{S}_1^{-1} \left(q_1 - \frac{1-\tau}{1+\tau} q_2 \right) + \frac{1}{1+\tau} \mathbf{T}^{-1} q_2 \end{Bmatrix} \quad (3)$$

where

$$\mathbf{S}_1 = \frac{-(1+\tau)\mathbf{S}}{\text{term 1}} - \frac{[(1-\tau)^2/(1+\tau)]\mathbf{T}}{\text{term 2}} + \frac{(1-\tau)\mathbf{R}}{\text{term 3}}. \quad (4)$$

It is evident that the efficient computation of (3) relies on the efficient solution of \mathbf{S}_1 and \mathbf{T} . The \mathbf{T} is a mass matrix, which is related to the inner product of vector bases. It can be solved in linear time with the same orthogonal finite-element reduction-recovery (OrFE-RR) described in [1]. The same is true for the weighted sum of \mathbf{T} and \mathbf{R} since \mathbf{R} has the same structure as \mathbf{T} . However, the \mathbf{S}_1 is a weighted sum of \mathbf{S} , \mathbf{T} , and \mathbf{R} . Since \mathbf{S} is formed by the *curl* of the vector bases, the resultant \mathbf{S}_1 cannot be solved in linear time by the same method in [1]. Next, we show how to solve \mathbf{S}_1 in linear complexity.

B. Efficient Iterative Solution of \mathbf{S}_1

\mathbf{S}_1 is, in general, not positive definite. Thus, the GMRES is the iterative method for choice. The iteration number of a GMRES solver typical grows with matrix size. Here, we develop an effective and efficient preconditioner \mathbf{M} as follows:

$$\mathbf{M} = -(1+\tau)\mathbf{S}_m - [(1-\tau)^2/(1+\tau)]\mathbf{T} + (1-\tau)\mathbf{R} \quad (5)$$

where \mathbf{S}_m is the component of \mathbf{S} that has the same structure as \mathbf{T} and \mathbf{R} . This structure is nothing but the matrix formed by the inner product of vector bases. Thus, we can directly apply the OrFE-RR method in [1] to solve \mathbf{M} in linear complexity. On the other hand, through the appropriate choice of τ , we can make \mathbf{M} an effective preconditioner as follows.

Since the preconditioning matrix \mathbf{M} consists of the same term 2, term 3, and one component of term 1 in (4), \mathbf{M} would dominate \mathbf{S}_1 if the norm of term 1 is smaller than that of the combined term 2 and term 3. Here, $\tau = (1 + j2\pi f_{\text{init}})/(1 - j2\pi f_{\text{init}})$, where f_{init} is the initial guess of the resonant frequency, which is the eigenvalue of (1) divided by $(j2\pi)$. Since τ is inside a unit circle regardless of f_{init} , we have a wide range to choose f_{init} to facilitate an efficient solution of \mathbf{M} without degrading the efficiency of finding eigenvalues of physical interest. Since $1 + \tau = 2/(1 - j2\pi f_{\text{init}})$ and $1 - \tau = (j4\pi f_{\text{init}})/(1 - j2\pi f_{\text{init}})$, if we increase the initial guess of f_{init} , the magnitude of $1 + \tau$ would become smaller and that of $1 - \tau$ would remain the same. As a result, term 1 will become smaller, and the combined term 2 and term 3 will become larger. And hence, by choosing a larger initial guess of f_{init} , \mathbf{M} can be made dominate in the \mathbf{S}_1 matrix, and thereby reducing the number of iterations required for the convergence of GMRES. How large f_{init} should be can be quantitatively analyzed based on the matrix norms of the three terms in (4), and then determined such that \mathbf{S}_1 is dominated by terms 2 and 3. Based on the physical dimension of on-chip structures, we found that when f_{init} is chosen higher than 10 GHz, we can achieve the same convergence performance in the GMRES-based iteration solution of \mathbf{S}_1 regardless of the problem size of the on-chip structures. Theoretically speaking, this is because $\mathbf{M}^{-1}\mathbf{S}_1$ has a bounded spectral radius irrespective of problem size. To see this point more clearly, let x be the eigenvector of $\mathbf{M}^{-1}\mathbf{S}_1$, and ξ be eigenvalues. We have $\xi = x^T \mathbf{S}_1 x / x^T \mathbf{M} x = 1 + x^T \mathbf{W} x / x^T \mathbf{M} x$, where \mathbf{W} is the difference between \mathbf{S}_1 and \mathbf{M} . Since \mathbf{W} is only related to

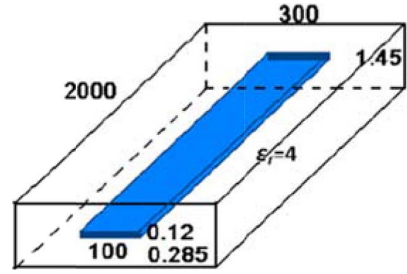


Fig. 1. On-chip stripline structure.

TABLE I
THE LOWEST RESONANT FREQUENCY SIMULATED WITH A DIFFERENT NUMBER OF ARNOLDI STEPS (UNIT: GHz)

# of Arnoldi steps	10	20	50	100	200	300 (Ref. [1])
Resonant frequency	51+j49	53+j59	53+j59	53+j59	53+j59	53+j59

the stiffness matrix, and the stiffness matrix is only related to permeability, the norm of \mathbf{W} does not change with problem size. On the other hand, the norm of \mathbf{M} is dominated by that of the conductivity-related \mathbf{R} , which has little dependence on the problem size either. \mathbf{M} 's norm over \mathbf{W} 's norm is proportional to $k^2 l^2 \sigma / (\omega \epsilon)$, where $\omega = 2\pi f_{\text{init}}$, k is the corresponding wavenumber, l is the average edge length, σ is metal conductivity, and ϵ is permittivity. Hence, the maximum modulus of ξ , thereby the spectral radius of $\mathbf{M}^{-1}\mathbf{S}_1$, has little dependence on the problem size. More important, with a choice of high f_{init} , the norm of \mathbf{W} over that of \mathbf{M} is small, and hence the eigenvalues of $\mathbf{M}^{-1}\mathbf{S}_1$ are very close to 1, thus making the iteration number small.

C. Performance Analysis

In the proposed eigenvalue solver, we transform the original eigenvalue problem (1) to (2), and also we shift the largest eigenvalues of (2) to be close to the eigenvalues of interest. As a result, we only need to perform $O(k)$ steps to find k eigenvalues of interest instead of using many Arnoldi steps. In each Arnoldi step, the computation of $\mathbf{B}'^{-1}\mathbf{A}'$ multiplied by a vector is performed in linear complexity as shown in (3) with the efficient solution of \mathbf{T} and \mathbf{S}_1 . As a result, the total complexity of the proposed eigenvalue solver is linear for finding k eigenvalues of interest.

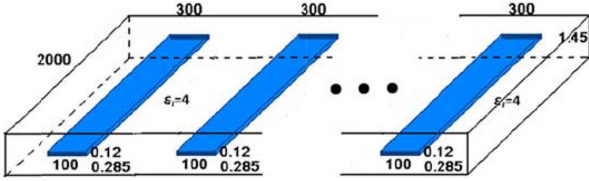
III. NUMERICAL RESULTS

A. On-Chip Stripline

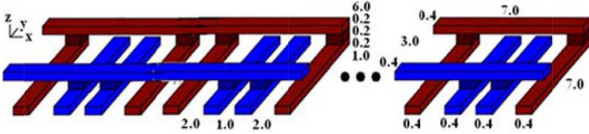
The single stripline structure, illustrated in Fig. 1, is simulated to examine the number of Arnoldi steps required to find the lowest complex resonant frequency. The dimension of the system matrix is 1 536, the conductivity is 5×10^7 , and the initial guess f_{init} is 100 GHz. Table I lists the computed lowest resonant frequency for different number of Arnoldi steps. The reference value is obtained from the solver in [1] with the same system matrices. The effectiveness of the proposed eigenvalue solver can be clearly seen from Table I. Even with 20 Arnoldi steps, we can obtain the desired eigenvalue, in contrast to the 300 used by the method in [1].

B. On-Chip Bus Structures

Next, we examine the number of GMRES iterations required in the proposed eigenvalue solver as the structure size increases. The previous single stripline structure is extended horizontally

Fig. 2. Illustration of on-chip bus structures. (unit: μm).TABLE II
GMRES ITERATIONS FOR THE BUS STRUCTURES

# of Unknowns	3,768	4,512	5,256	6,000	6,744	7,488
$N_x N_y N_z$	4, 16, 4	4, 19, 4	4, 22, 4	4, 25, 4	4, 28, 4	4, 31, 4
$K(\mathbf{S}_1) (\times 10^7)$	3.29	3.29	3.29	3.29	3.29	3.29
$K(\mathbf{M}) (\times 10^7)$	5.17	5.17	5.17	5.17	5.17	5.17
Spectral Radius	1.553	1.553	1.553	1.553	1.553	1.553
# of iteration	36.2	36.1	36.1	36.0	36.0	35.9

Fig. 3. On-chip power grid structure. (unit: μm).

to a multi-line bus structure as shown in Fig. 2. It can be seen from Table II that, with the proposed preconditioner, the required number of iterations is kept to be a constant in the entire range of problem sizes. Here, the f_{init} is chosen as 10^{12} Hz, the number of Arnoldi iterations is 200, and the tolerance in GMRES convergence is set as 10^{-6} . The iteration number shown in Table II is the average iteration number of the GMRES solution in the 200 Arnoldi steps of the eigenvalue solution. Table II also shows that the spectral radius of $\mathbf{I} - \mathbf{M}^{-1}\mathbf{S}_1$, $\rho(\mathbf{I} - \mathbf{M}^{-1}\mathbf{S}_1)$, for all cases is a bounded constant, and the eigenvalues of $\mathbf{M}^{-1}\mathbf{S}_1$ are distributed in a circle of radius 1.553 centered around one. In addition, the condition number of \mathbf{S}_1 and that of the preconditioning matrix \mathbf{M} , denoted by $K(\mathbf{S}_1)$, and $K(\mathbf{M})$ respectively, are shown to be constant although the structure is enlarged. As a result, the iteration number required for GMRES convergence is shown to be constant regardless of the number of buses included in this example.

C. On-Chip Power Grid Structures

We also examine the performance of the proposed iterative solution of \mathbf{S}_1 with multiple power grid structures shown in Fig. 3. The relative permittivity for each layer is 3, 4, 3, 4, and 3.5 from bottom to top. The initial guess f_{init} is 30×10^{12} Hz. The number of Arnoldi iterations is 200 in contrast to 1000 used in [1], and the tolerance in GMRES is set as 10^{-6} . In Table III, the GMRES iteration numbers are listed with respect to the size of the power grid structure. The $K(\mathbf{S}_1)$, $K(\mathbf{M})$, and the spectral radius ρ are also shown to be constant regardless of the structure size. To demonstrate that the effectiveness of the proposed preconditioner is not due to the periodicity of the structure, we also simulate an irregular power grid as shown in Fig. 4. The result is shown in the last column of Table III. Despite the difference in layout and its non-periodicity, we observe similar values in the matrix condition number, the spectral radius of $\mathbf{M}^{-1}\mathbf{S}_1$, and the GMRES iteration number.

D. Performance Comparison

We compare the CPU time of the proposed eigenvalue solver with Matlab. In Fig. 5, the CPU time is plotted for the power

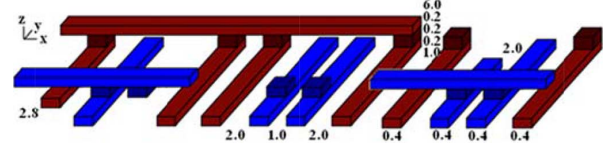
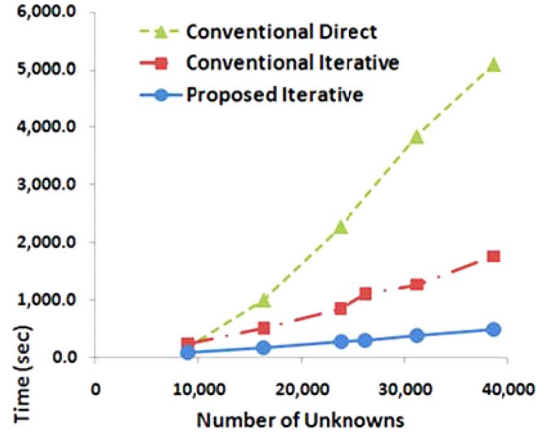
Fig. 4. Irregular power grid structure. (unit: μm).

Fig. 5. CPU time comparison for the power grid structures.

TABLE III
GMRES ITERATIONS FOR POWER GRID SIMULATION

	1 unit	2 units	3 units	4 units	5 units	Irregular
# of Unknowns	8,904	16,320	23,736	31,152	38,568	26,208
$N_x N_y N_z$	12, 8, 6	12, 14, 6	12, 20, 6	12, 26, 6	12, 32, 6	12, 22, 6
$K(\mathbf{S}_1) (\times 10^7)$	10.1	10.1	9.99	10.0	10.1	10.2
$K(\mathbf{M}) (\times 10^7)$	1.88	1.88	1.88	1.88	1.88	1.88
$\rho(\mathbf{I} - \mathbf{M}^{-1}\mathbf{S}_1)$	1.381	1.381	1.381	1.381	1.396	1.396
Iteration No.	64.8	64.6	64.0	63.9	64.2	65.2

grid example as the dimension of the system matrix increases. The three lines in Fig. 5 represent the time cost by the Matlab's eigenvalue solver that employs a direct sparse solver for computing $\mathbf{B}'^{-1}\mathbf{A}'q$, the Matlab's eigenvalue solver that employs a GMRES-based iterative solution of $\mathbf{B}'^{-1}\mathbf{A}'q$ with the proposed preconditioner, and the proposed eigenvalue solution with a linear-complexity solution of $\mathbf{B}'^{-1}\mathbf{A}'q$, respectively. The proposed solution is shown to outperform the other two solutions. In addition, a clear linear scaling is observed.

IV. CONCLUSION

This letter presents a finite-element-based eigenvalue solver of linear complexity for analyzing 3-D on-chip integrated circuits consisting of lossy conductors and inhomogeneous dielectrics. Numerical results have demonstrated the accuracy and efficiency of the proposed solver.

REFERENCES

- [1] J. Lee, D. Chen, V. Balakrishnan, C.-K. Koh, and D. Jiao, "A quadratic eigenvalue solver of linear complexity for 3-D electromagnetics-based analysis of large-scale integrated circuits," *IEEE Trans. CAD*, vol. 31, no. 3, pp. 380–390, Mar. 2012.
- [2] R. B. Lehoucq, "Analysis and Implementation of an Implicitly Restarted Arnoldi Iteration," Ph.D. dissertation, Rice Univ., Houston, TX, 1995.
- [3] J. R. Brauer and G. C. Lizalek, "Microwave filter analysis using a new 3-D finite-element modal frequency method," *IEEE Trans. Microw. Theory Tech.*, vol. 45, no. 5, pp. 810–818, May 1997.
- [4] L. N. Trefethen and D. Bau, *Numerical Linear Algebra*, 1st ed. Philadelphia, PA: SIAM, 1997.
- [5] F. Zhang, *The Schur Complement and Its Applications*. New York: Springer, 2005.